(a) **Impact of mechanical deformation on pseudo-ECGs: a simulation study**

(b) M. Favino[1], S. Pozzi[1], S. Pezzuto[1],
F. Prinzen[2], A. Auricchio[3], R. Krause[1]

(c) Center for Computational Medicine in Cardiology (CCMC);

Institute of Computational Science (ICS),
Università della Svizzera italiana;

Department of Physiology,
Cardiovascular Research Institute Maastricht (CARIM).

(d) [1] Institute of Computational Science,
Università della Svizzera italiana,
Via Giuseppe Buffi 13, CH-6900 Lugano, Svizzera

M. Favino	Phone: +41 (0) 58 666 49 71	Email : marco.favino@usi.ch
S. Pozzi	Phone: +41 (0) 58 666 49 72	Email: sonia.pozzi@usi.ch
S. Pezzuto	Phone: +41 (0) 58 666 49 75	Email: simone.pezzuto@usi.ch
R. Krause	Phone: +41 (0) 58 666 43 09	Email: rolf.krause@usi.ch

[2] Department of Physiology,
Cardiovascular Research Institute Maastricht (CARIM),
Universiteitssingel 50, 6229 ER Maastricht, The Netherlands

F. Prinzen Phone: +31 43 3881080 Email: frits.prinzen@maastrichtuniversity.nl

[3] Division of Cardiology,
Fondazione Cardiocentro Ticino,
Via Tesserete 48, CH-6900 Lugano, Svizzera

A. Auricchio Phone: + 41 91 805 3340 Email: angelo.auricchio@cardiocentro.org

(e) Marco Favino,
Institute of Computational Science,
Università della Svizzera italiana,
Via Giuseppe Buffi 13, CH-6900 Lugano, Svizzera

Phone: +41 (0) 58 666 49 71 Email : marco.favino@usi.ch

Abstract

Aims Heart failure is often accompanied by abnormal propagation of electrical signals. Electrophysiological simulations have become a key tool to investigate causes and possible treatments of heart failure. In order to describe the physiology of the heart as realistic as possible, electrophysiological models can be enriched by means of a mechanical model, thus taking the deformation occurring during of cardiac activity into account. In our work, we use an electro-mechanical model in order to study the effect of mechanical deformation onto the results electrophysiological simulations.

Methods We investigated the pseudo-ECGs arising from the propagation of electrical signals in a tissue slab undergoing active mechanical deformation. We used the mono-domain equation for electrophysiology with the Bueno-Orovio ionic model. For the mechanics, we employ a fully incompressible Guccione-Costa hyperelastic law and the Panfilov model for the active force. We compare the purely electrophysiological approach with mono- and bi-directional electromechanical coupling strategy.

Results Each scenario leads to a specific activation pattern and mechanical deformation and, consequently, pseudo-ECGs. T-wave amplitude changes are observed in all the experiments. QRS complex is also affected under specific circumstances mostly related to the dimensions of the tissue slab, the fibre orientation and the electrode position. Surprisingly, purely electrophysiology setting provides a better approximation to the most realistic bi-directional coupling than the mono-directional coupling, although the physical explanation is not straightforward.

Conclusions Activation and ECG are not trivially affected by the mechanical deformation. Possible changes in QRS complex may be due to the approximation strategy rather than the underlying physiology.

Keywords

Electro-mechanical computational model; Pseudo-ECG; T-wave morphology; notching in QRS-complex;

Deleted: one of the most common causes of death in developed countries. It is

Deleted: this disease

Deleted: Our study is performed in terms

Deleted: of

Deleted: with

Deleted: stress

Deleted: consider

Deleted: three scenarios:

Deleted: directional

Deleted: coupling,

Deleted: and pure electrophysiology.

Deleted: The three different scenarios lead to different activation patterns

Condensed abstract

This study shows that ECG is non-trivially affected by the mechanical deformation. A purely electrophysiological approach was compared to the mono- and bi-directional coupling of electrophysiology and mechanics. The numerical experiments showed an impact of mechanics on the T-wave and, under specific circumstances, on the QRS complex as well.

Deleted: how

Deleted: is

Deleted: that

Deleted: is mostly affected,

Deleted: that changes in the

Deleted: may occur under specific circumstances.

What's New?

1. Computation of pseudo-ECGs properly accounting for the mechanical deformation.
2. Comparison of three different cardiac electrophysiology model with increasing level of complexity in handling geometrical changes due to mechanics.
3. Sequential computation of activation and then deformation of the tissue showed non-physiological artefacts in the pseudo-ECG with respect to a fully coupled approach.
4. In same cases, QRS-complex presented notching if the contraction started before the tissue had been fully activated.

Deleted: s

Deleted: may

Deleted: s

Deleted: s

Introduction

The spatio-temporal morphology of the electrocardiogram (ECG) is the result of the electric and mechanical activity of the heart within the torso. Most of the electrophysiology studies encodes only the relative motion of the extracellular action potential with respect to the position of the electrodes. Based on this first approximation, nowadays, patient-tailored ECGs can in principle be simulated in a few minutes on high performance computing (HPC) architectures with anatomically detailed cardiac electrophysiology models [1]. This is possible once a fixed geometry and given model parameters are available, but these pure electrophysiological models do not account for any mechanical effect, since the simulations run on a static geometry.

In fact, the heart is mechanically active, yielding to a complex multi-physics problem spanning several temporal and spatial scales. Thanks to the increasing computing power, only very recently, its numerical simulation has become feasible [2,27,28] and it is becoming always more accepted that, also the myocardium deformation which influences the ECG morphology in particular the T-wave, have to be considered and included [3]. This allows to model and simulate the complex superposition of the transmembrane potential evolution relative to a static configuration, which is usually used in stand-alone electrophysiological simulations, and the motion of the wall relative to the ECG lead.

Effects of geometrical changes in cardiac electrophysiology have been considered only in a very few works.

In [4], dependence of ECGs on geometrical deformations has been studied in a two-dimensional case, where a section of a torso was considered. In this work, the mechanics of the torso was also considered but mechanical deformations were not coupled with the bi-domain model.

In [3], a "static-dynamic" approach has been employed. The static step consists in the solution of a mono-domain system on a reference geometry. Then deformations are applied on the geometry in order to evaluate the ECGs.

In [5], a model for a fully coupled electro-mechanical system has been presented. There, the mechanical activation depends on trans-membrane potential. Because of boundary and initial conditions, the considered case is a tissue wedge that can move only in a two-dimensional plane, even if simulations are performed in a three-dimensional setting.

Finally, in [6] a comparison of ECGs has been performed on a realistic heart geometry comparing systolic and diastolic configurations. Even if no dynamical effect is considered, variations can be observed in resulting signal.

In all this works, changes in amplitude and in peak of the T-wave were observed.

The aim of this paper is to investigate the impact of the mechanical deformation of a tissue slab on the pseudo-ECG by means of a multi-scale computational model. In particular, we compare three different scenarios: purely electrophysiological, mono-directional electro-mechanical coupling and bi-directional coupling. The first scenario does not include any mechanical effects and it is our reference solution. The second and third scenarios both include the deformation. In the second one the electrophysiological problem does not account for any change in the parameters due to the deformation, similarly to the "static-dynamic" approach. This second scenario is computationally appealing since electrophysiology and mechanics can be solved sequentially. Finally, the last scenario includes the mechano-electric feedback, which significantly increases the computational complexity.

To this purpose, we developed a novel numerical algorithm, which solves the strongly coupled problem on two distinct computational meshes, one for the mechanical problem and the other for the electrophysiological one. Indeed, while the mechanics can be solved on a relatively coarse grid, a very fine mesh is necessary in order to capture the steep gradients arising in the action potential propagation [7]. Our solver is based on massively parallel variational transfer that enables seamless communication between the two grids [8], [9].

To our knowledge, the present study is the first one in which effects of mechanics are studied in a real three-dimensional case.

Deleted: 2

Deleted: 3

Deleted: 1

Deleted: 1

Methods

Mathematical model

The bi-domain equation describes the evolution of intra- and extra-cellular potential in the cardiac tissue. It can be formally derived from a macroscopic conservation of charges and suitable constitutive relationships. More rigorously, although under simplifying assumptions, the bi-domain model can be obtained by homogenization, as mean-field equations of balance laws at the cellular spatial scale [10]. In this work, we employ the former approach since, as in similar multi-phasic theories such as poro-elasticity [11], it allows to naturally extend these models on moving domains. Following the majority of the literature, we assume the mono-domain approximation, which decouples the evolution of the transmembrane potential from the extra-cellular potential evaluation, allowing for a significant computational burden reduction.

In order to derive the mono-domain equation in a moving domain, we followed the strategy presented in [12]. Mono-domain system is mapped into the reference configuration by means of the deformation gradient tensor $\boldsymbol{F}$. Hence, the modified conductivity tensor reads $\boldsymbol{F}^{-1}\boldsymbol{G}_{mono}\boldsymbol{F}^{-T}$, which is the Piola transformation of the conductivity $\boldsymbol{G}_{mono}$. In this way, we included changes in the parameters only due to geometrical deformations. We did not consider possible variations due to the change of micro-structure [13].

The mono-domain system is coupled with the incompressible, anisotropic, hyperelastic mechanical model presented and validated in [14]. It is worth to remark that, differently from several other models from the literature [12,15,3], we assumed the cardiac tissue to be fully incompressible. This assumption is commonly accepted for biological tissues, since the main constituent is water, which is an incompressible fluid. This constraint is enforced exactly and not by penalization, hence at each time-step a non-linear saddle-point system has to be solved. This poses significant difficulties from a computational standpoint. Material is supposed to be orthotropic both in the mechanical and in the electrophysiological part. The passive stress is described by the Guccione-Costa strain-energy density function [16]. Since the material is assumed to be fully incompressible, a splitting between the deviatoric (shear) and volumetric deformation is introduced into the model [17].

In order to couple the mechanical system with the mono-domain equation an active stress approach has been employed [12], [14] and [15]. The active force is exerted only along the fiber direction. The temporal evolution of the force generated by myocytes is described by the model introduced in [15]. In this simplified model, the active force depends only on a scaled trans-membrane potential which is multiplied by a prescribed maximum active force T_a^{max}. This model does not account for neither Frank-Starling's nor Hill's effects.

Computation of pseudo-ECG

The surface ECGs requires the solution of the bi-domain equation in the torso for each time-step, which is in general computationally expensive. Since ECGs have to be computed only at specific locations, this computation may be reduced to the evaluation of the dot product between the trans-membrane currents and a so-called lead-field (or Green's functions) for each electrode. When considering the fully-coupled electro-mechanical problem, this strategy is not applicable, because the lead-field varies over time due to geometry and coefficients changes.

In this work, we introduce two hypotheses to recover feasibility of the lead-field approach. We assume that:

Deleted: 3

Deleted: 7

Deleted: 2

Deleted: 3

Deleted: 4

Deleted: 5

Deleted: 6

Deleted: 2

Deleted: 3

Deleted: 4

Deleted: 4

1. the tissue slab is immersed into a physiological bath significantly bigger than the slab itself. We also suppose that the embedding fluid is not viscous. This can be interpreted as an infinite torso with zero stiffness [18];
2. limited to the lead-fields computation, the electrical conductivity of the cardiac tissue and the physiological bath are equal. This approximation is valid in the case of electrodes far from the cardiac tissue.

Under these assumptions, we can extend the formula presented in [19] on a deformed domain, i.e.

$$E(X') = \int_{\Omega} \boldsymbol{F}^{-1}\boldsymbol{G}_{mono}\boldsymbol{F}^{-T}\nabla V(\mathrm{X}) \cdot \nabla\varphi(\mathrm{X} - \mathrm{X}')\mathrm{dX}.$$

Hence, the actual computation of the pseudo-ECGs is realized on the reference configuration Ω by employing the Piola transformation and does not require the re-computation of the lead-field.

Computational domains, model parameters, and electrode locations

In general, computation of electrophysiological quantities depends on the interaction of several factors, i.e. geometry, position of the heart, interaction with the blood, position of the heart, and so forth. Since we aim to systematically study the effect of the mechanical deformation on ECGs, we reduce the complex effects due to geometry, considering as domains two different computational slabs. In particular, we consider three test cases:

A. a cube with edge of 0.7 mm and fibers aligned along x-axis,
B. a slab of size 20 mm × 7 mm × 3 mm and fibers aligned along x-axis,
C. a slab of size 20 mm × 7 mm × 3 mm and fibers aligned along y-axis.

The test case (B) is the electro-mechanical enrichment of the purely electrophysiological test studied in [20]. The electrophysiological parameters are as in this latter work and in order to remove rigid body motions, the three faces along the planes x = 0, y = 0, and z = 0 are fixed in the normal direction.

The parameters for mechanics are from [14]. Gating variables have been described by a Bueno-Orovio model [21]. In this model, different parameters are introduced in order to appropriately fit epi-, M-, and endo-cardial cells. Here, we used a single set of parameters for the cellular model, i.e. the endo-cardial one. For what concerns the active force model [15], the time relaxation constant has been set to $\varepsilon = 10$ ms $^{-1}$. Here, a value of T_a^{max}=47.9 N×m $^{-2}$ was suggested as maximum active force. After a systematic analysis of the effects on this parameter, for $T_a^{max} = \{10$ kPa, 20 kPa, 30 kPa, 40 kPa, 47.9 kPa $\}$, we set its value to T_a^{max}=30 N×m $^{-2}$. The other values gave numerical instabilities in the mechanical solver and they are detailed presented in the Discussion section.

We consider six unipolar electrodes $\boldsymbol{E}_{i,\pm}$ in total, two for each Cartesian axis $i = \{x, y, z\}$. They are arranged symmetrically with respect to the centre of the domain and are 10 cm apart from the boundary faces. In addition, the unipolar signals from electrodes aligned in the same direction are combined into a single bipolar ECG, with the electrode in the positive direction being the cathode and the opposite one being the anode, defining $\boldsymbol{E}_{i,} = \boldsymbol{E}_{i,+} - \boldsymbol{E}_{i,-}$.

Discretization and solution

Deleted: 22

Deleted: 23

Deleted: 18

Deleted: 2

Deleted: 19

Deleted: 4

The multi-scale nature of the electro-mechanical problem allows to employ different spatial and temporal meshes. In literature, this fact usually exploited introducing staggered solvers that iteratively solve first one problem and then the other one [22], [12].
On the other hand, this approach requires suitable projection operators in order to exchange data between the two computational domains.

The model presented in the previous sections has been implemented in the finite element (FE) framework MOOSE [23]. Inside this package, we implemented HART, an application for simulation of cardiac electro-mechanics. The fully-coupled iterative scheme is summarized in Fig. 1. At each time-step, we first transfer the deformation from the coarse mechanical mesh to the fine electrophysiology mesh. Using the deformation at previous time step, we compute the ionic currents by means an explicit scheme. These are then used to update the potential at the new time step that is then transferred to coarse mesh. Here the new active force is computed by means of the Panfilov model and finally the new deformation is computed.

Time integration of the mono-domain system has been performed by means of an implicit-explicit (IMEX) scheme. Gating variables are explicitly integrated employing a Rush-Larsen scheme and the resulting currents are used as a source term for the diffusion problem. For this latter, we adopted an implicit Euler scheme. The non-linear mechanical model has been solved with Newton's method. Globally, the numerical scheme converges linearly with respect to the time-step and quadratically with respect to the mesh size.

The linear system arising from the IMEX linearization of the non-linear mono-domain equation has been solved with an algebraic multigrid solver (BoomerAMG) and the linear system arising from non-linear mechanics has been solved with a parallel direct solver (SuperLU).

Validation and choice of discretization parameters

The presented mechanical model has been validated in [14], where a comparison between different implementations of mechanical solvers has been performed. In order to check the accuracy of the electrophysiology solver, we performed a convergence analysis on ECGs signals under uniform refinement of the spatial grid and of the time-step size.
The convergence tests are performed using case C setup, in which fibres are aligned along the y-axis. We impose homogeneous boundary conditions for the flux. The time window is 600 ms.

First, the convergence with respect to the spatial mesh-size has been studied employing three different uniform grids E_c, E_m and E_f, respectively, of mesh-size 0.5 mm, 0.25 mm, and 0.125 mm. A temporal step-size $\boldsymbol{t_f}$ = 0.0125 ms has been used. The obtained results are reported in the top row of Fig. 2. We observe convergence of the shape of the unipolar pseudo-ECGs under spatial mesh refinement. Numerical instabilities observed with the mesh E_c are reduced with the use of E_m, and disappear completely with the use of E_f.
It is interesting to notice that a longer QRS complex in the pseudo-ECG is observed for smaller mesh-size. In our numerical code, the coarser the mesh-size, then slower the conduction velocity, which is consistent with a FE discretization, in contrast to a finite difference (FD) approach that would have produced the opposite effect [7].

Secondly, the convergence with respect to the temporal step-size has been studied employing three different temporal grids, of lengths t_c =0.05 ms, t_m =0.025 ms, and t_c = 0.0125 ms. The coarsest step-size has been chosen in order have a stable behavior in the numerical integration of the gating variables. The employed spatial grid is $\boldsymbol{E_f}$. The obtained results are reported in the bottom row of Fig. 2. We observe a convergence of the pseudo-ECGs under temporal mesh refinement. Differently from the previous test, small step-lengths give larger conduction velocities.

Deleted: 0
Deleted: 3
Deleted: 1
Deleted: 2

The performed validation tests suggest that the grid $\boldsymbol{E_f}$ and the step-size t_c are suitable to capture pseudo-EGCs behaviour and hence they have been chosen for the following numerical tests. This choice also provides a trade-off between the numerical accuracy of the electrophysiology solver and its computational cost.
Since no steep gradients in the deformation are usually present, the mechanical solver instead employs a coarser mesh of step-size 0.5 mm and the same time-step size of the electrophysiology solver.

Results

The model, discretization, and solution algorithm presented in the previous sections have been used to compute pseudo-ECGs under three different computational scenarios:

1. Pure electrophysiology (green line): this is the standard setting usually employed in literature for the computation of ECGs. From the model previously presented, it is obtained by neglecting the change of conductivities due to the change of the geometry.

2. Mono-directional coupling (or static-dynamic approach, red line): mono-domain system is solved on a fixed configuration as in the previous setting. The resulting potential is then employed to compute the active force and the current configuration. This deformed configuration is finally employed to compute pseudo-ECGs. From the complete model, this scenario can be obtained by neglecting the change of conductivity only in the electrophysiology solver.

3. Bi-directional coupling (blue line): the mono-domain system is solved on a deformed configuration. As for the previous case, pseudo-ECGs are computed on the current configuration. We consider variations of the conductivity and fiber directions due to geometrical deformations.

From a mathematical standpoint, the first setup can be obtained by setting the deformation gradient to the identity tensor both in the electrophysiology solver and the computation of the ECGs. Instead, the second setup can be obtained by neglecting the Piola transformation only in the computation of the potential. Hence, in the first two setups the activation map is the same but different configurations have been employed to compute ECGs.
These computational scenarios have been used to compute bipolar ECGs along the three coordinate axes for the three test geometries described in the previous section.

Test Case A

This test case has been chosen to remove geometrical effects. Fibers are aligned along the x-axis and, hence, the same propagation is expected along the other two coordinate axes. In Fig. **3,** different snapshots of the depolarization phase are reported for the mono-directional (top row) and the bi-directional (bottom row) approaches. Different propagation patterns are obtained with these two settings. In the mono-directional coupling, the propagation front remains elliptic while, due to the changes in the conductivity, a flatter front is observed in the fully-coupled scenario. This latter approach is also expected to give a faster signal along fiber direction, due to the changes in the conductivity and the contraction of the geometry.
Actually this can be observed in the first row of Fig. 5. The fully-coupled approach gives a faster QRS complex although the difference cannot be fully appreciated since the deformation is small during the depolarization phase.
Along fibers, we observe largest changes in the signal. At the end of the QRS complex we observe larger values for the potential and smaller values in the T-wave. In the cross-fibre direction no

differences are observed in the QRS complex and smaller potentials are observed in the T-wave. The largest differences are observed between Setting 2 and the other approaches.
In fact, in the mono-directional coupling, we observe a notching in the ECG signal from electrodes along the contraction direction. As expected, along y- and z-axis signals are the same and no significant differences are visible between the three scenarios. Hence, the pure-electrophysiology case can be considered a good approximation of the fully-coupled approach in the cross fibre directions.

Test Case B

The other two test cases have been employed to introduce also the dependency of ECG signals on the geometry. In this second test, the tissue slab has fibers aligned along the x-axis. A remarkable contraction occurs in the direction of the fibers. The discrepancies noticed in Case A. between the propagation front for the mono-directional and for the bi-directional approaches are also observed in this case even if weakened.
See Fig. 5. (second row) to see the obtained pseudo-ECGs. In this test, we do not observe large variations in the QRS complex for ECGs in the three directions. Changes can be observed in the T-wave: larger potentials are observed along the longitudinal axis, smaller potential are observed along the medium axis, and a change in sign along the short axis. In this latter case, we also notice a delay in the T-wave.
Since no preeminent information concerning the QRS complex arise from this test case, snapshots related to the different depolarization phase are omitted for this test case.
We also noticed that mechanics may also be responsible for change of sign of the repolarization wave. This has been observed in particular along the z-axis, where the transmural direction is short and a large thickening happens. This result has not been reported since, for leads close to the geometry, the employed Green's function does not provide a good approximation of the realistic lead field but this observation may be worth of further investigations.

Test Case C

Finally, in order to understand if the notch reported in test case A depends on a combination of domain size and fibres direction, we reproduced the same experiment reported in test case B but with fibers aligned along the medium axis (y) direction. As reported in Fig. **4**. the tissue preparation contracted along y-axis, so that the tissue approached the electrodes in the x direction.
This set-up confirmed the results of case A. Differences in the propagation of the activation front between the mono-directional and the fully-coupled approaches are comparable to the ones observed for test case C. Third row of Fig. 5 reports the obtained pseudo-ECGs. Along y-directions, differences both in QRS complex and in the T-wave can be observed between the coupled model and the purely electrophysiological one. The coupled model provides larger signals at the end of the depolarization phase and small signals in the repolarization phase. Differently from test case B, no large differences can be observed in the short axis direction.

Impact on conduction velocity

To study the impact of tissue deformation on the conduction velocity, we eventually compared the activation time at several points along the diagonal connecting the early activation site with the opposite vertex. The variations in the activation time due to geometry changes are reported in Tab. 1. Because of the definition of our settings, pure-electrophysiology and mono-directional coupling provide the same activation times.
Along the selected segment for test cases A and C an elongation of the tissue is observed while for test case B a contraction is observed. For this reason, for the former ones a delay in the activation is expected while for the latter one an earlier activation is expected (for the fully-coupled approach with respect to the mono-directional coupled approach).

Expectations are respected for test cases A and C. These differences are due to a noticeable effect on the conduction velocity.

Discussion

In most of works in the literature, ECGs are usually computed as static processes, without considering the mechanical deformation due to the beating heart and breathing. The presented systematic comparison shows that different ways of coupling electrophysiology and cardiac mechanics may result in different propagation patterns and ECGs. We confirmed the preliminary results of the few, to the best of our knowledge, works that accounted for the effects of mechanics on extra-cardiac electrical signals, i.e. a delay in the T-wave [4], a smaller amplitude of the T-wave [1,5], and possibly changes in the QRS complex [6].
In order to focus only on the effects of the mechanical deformation on the pseudo-ECG, we reduced the complexity of the model by employing two simple geometries: a cube and a slab. We did not consider any other mechano-electric feedback mechanisms. Microstructure was homogeneous and directed along the coordinate axes. Since one cell type was considered, the reference action potential was homogeneous across the tissue; in this respect, T-wave is expected to be discordant to the QRS-complex. This was indeed confirmed by the results presented above.

A significant impact of the deformation on pseudo-ECG was also due to: relative position of electrodes with respect to the domain, domain size, and fibre directions. In general, test cases A and C confirmed that if the dimension along the fibre direction is not large enough, differences can be observed in the QRS-complex and in the T-wave. Instead, in test case B, if the dimension along the fibre direction is long enough, differences are more relevant in the T-wave. Pure electrophysiological systems give in general larger potentials.

In many cases, the mono-directional coupling provided a good approximation of the fully-coupled system. Moreover, the computational burden was significantly reduced by assuming mono-directional coupling.

Notching and impact on local conduction velocity

The use of the mono-directional coupling resulted in some cases in ECG signals characterized by a notch that was not visible in the pure electrical simulations. This happened since the "static-dynamic" approximation was not sufficient in particular cases. On the other hand, notching reduced when a fully-coupled solver was used.

In the real ECG, presence of notching in specific ECG leads may be correlated to bundle branch block. For instance, in Left Bundle Branch Block (LBBB) patients the Purkinje conduction system in the left ventricle (LV) is not working properly, and thus the activation front comes from the right ventricle (RV). In the respect, notching could be a consequence of the slow trans-septal conduction.

Our experiments provided a possible additional explanation for notching in LBBB patient. LBBB is accompanied by a ventricular dyssynchrony, since the RV is activated first, and later the LV. The septum, which separates RV and LV, undergoes a complicated deformation, the so-called "septal flash", which has been reported and documented by several studies [24]. If the septum is deforming while the action potential is traveling through it from the RV to LV, the local conduction velocity may be affected. Moreover, the ECG lead may measure a backward motion of the extra-cellular potential with respect to the RV to LV direction, because the measure is always relative to the deformed configuration. In other words, if the action potential is traveling from the RV to LV within the septum, while the septum itself is moving faster than the propagation in the opposite direction, the overall motion is backward, and notching appears. This is occurring, for example. in the first and third rows of Fig. 5. In this experiments, propagation is orthogonal to the fibers, and thus the cube or the slab start to contract before the entire block has been activated. Because of

Deleted: s
Deleted: allowed to
Deleted: may be observed
Deleted: i
Deleted: is
Deleted: is
Deleted: is
Deleted: is
Deleted: s
Deleted: is
Deleted: ¶
Large differences between mono-domain on fixed and moving domain wereare observed closed to clamped faces. If we consider our computational domain as a wedge extracted from a ventricle, differences would be more visible in an ideal electrode inside the ventricular cavity then in a ventricle posed on the torso surface.¶
Deleted: is
Deleted: s
Deleted: is
Deleted: s
Deleted: i
Deleted: The

the incompressibility of the material, a contraction in the fiber direction translated into an expansion in the cross-fiber direction, introducing a relative motion of the action potential with respect to the electrodes.

Stability issues

As discussed in the choice of the parameters, in some case we observed an unstable behaviour of the mechanical solver. It is still unclear to us whether this was an intrinsic mathematical instability of the model or an issue of the numerical solver. The instability generally occurs during the repolarization phase, and it was due to a singularity in the linearized mechanical problem. This kind of problem has been reported by others in the literature [25], [26].
From a mathematical viewpoint, a possible source of instability is a lack of rank-one convexity of the Guccione-Costa hyperelastic material. Indeed, strain-energies defined with respect to the Green strain tensor, such as Fung-type materials, are in general not rank-one convex. The lack of rank-one convexity implies a singularity in the linearized mechanical problem, which is consistent to what we observe. In this case, an alternative is to switch to invariant-based material laws, for which rank-one convexity can be readily checked.
Another source of instability could come from the interplay between the hyperelastic law and the active force generation. Other groups observed instabilities in this respect but mostly associated to the velocity-dependent term of the active force (Hill's effect), which we do not consider in this work. In our case, it is possible that the contraction of the fibers due to the active force is reducing the stability of the system. It is well known that, in a hyperelastic material, fibres withstand forces only under extension, and that buckling may occur under compression. In a real heart, this should not happen because the ventricles are inflated right before systole, and thus fibres are already extended and ready to bare the active force.
From a numerical standpoint, the usage of different meshes for mechanics and electrophysiology introduces the necessity of a stable communication between the two grids. The orthogonal L^2-projection is known to be stable in this respect. In our tests, active force is a smoothed version on the action potential, which has a very steep gradient in the depolarization phase. It might be that under particular circumstances the mechanical grid is too coarse to capture the upstroke of the active force, thus the orthogonal L^2-projection introduces spurious oscillations which the lead to the instability. Although we believe this scenario is very unlikely, it is worth to mention since the staggered mesh approach has not been explored in depth yet.

Limitations

The model adopted in this paper comes with significant simplifications. The mechano-electric coupling (MEC) in the heart is a very active area of research, and several mechanisms should nowadays be included in physiologically motivated simulations. On the other hand, this work focussed on the impact deformation on the ECG from a purely geometrical point of view, which becomes hard to establish if several MEC mechanisms are included into the model.

The active force generation is also very basic and not well integrated into the cellular model, but we believe that this does not invalidate the results. Indeed, while more sophisticated active force models might lead to a different pseudo-ECG under similar experimental settings, the difference between pure electrophysiological, mono-directional and fully-coupled approaches would most likely be same as we observed, corroborating our findings.

On the other hand, the tissue slab geometry adopted in this paper, as well as the pseudo-ECG, is only a mere approximation of the heart-torso geometry and the 12-lead ECG. Further investigations on realistic geometries are necessary.

Finally, to the best of our knowledge, there is no rigorous derivation of the bi-domain equation on deformable tissues [13]. In principle, the pull-back in the reference configuration of the bi-domain equation should be done before the homogenization procedure, and not after. The parameters of

Deleted: i
Deleted: i
Deleted: 6
Deleted: 7
Deleted: filled
Deleted: 7

the bi-domain equation are effective and they solve a so-called "cell problem". This latter is not a static problem, if deformation is involved. In practice, the parameters are estimated a-posteriori from the conduction velocity but, with the deformation, this procedure is not entirely satisfactory. Further investigations are required in this respect.

Conclusions

We presented a coupled model for the electro-mechanics in the heart. The model accounted both for geometrical mechano-electric effects and the electro-mechanical coupling by means of an active stress strategy. We compared simulations performed with a fully-coupled model to simulations realized with two simplifications that are usually adopted in literature, i.e. the mono-directional coupling (or "static-dynamic" approach) and the pure-electrophysiological case. These two latter approaches, which allow to simplify the solution process, are actually simplification of the fully-coupled model.

The computational experiments presented in this paper highlighted a non-trivial impact of the mechanical deformation on the ECG. Beside the known effects on the delay and amplitude of the T-wave, which were present in almost all the simulations, significant changes were also observed in the QRS complex. These changes were observed in particular along the fibers direction if the thickness along this axis was not sufficiently large. Since we used simple axes-aligned geometries, ECGs along fiber direction are basically dominated by the activated area orthogonal to fiber direction. Short geometries give a complicated superposition of the activation of these two faces, while is the geometry is long enough, the two activations are basically decoupled.

Although the mono-directional coupling provides a first extension, it gave larger differences with respect to the pure-electrophysiology rather than the fully coupled model. This is explained by an inconsistency between the undeformed conductivity tensor and the deformed geometry employed for the computation of the ECGs.

We also point out large differences in the QRS-complex, introduced by the mono-directional coupling. These may suggest a possible mechanism for the notching observed in LBBB patients.

Further investigations are necessary, in order to understand the role of fibers distribution, e.g. employing slabs with non-uniform fiber directions, and of the geometry, e.g. employing a truncated ellipsoid or realistic heart.

Deleted: correct

Deleted: for

Deleted: effects

Deleted: the

Deleted: problem

Deleted: ,

Deleted: with

Deleted: and

Deleted: was

Deleted: giving

Deleted: basically

Deleted: these

Deleted: and due to an inconsistent conductivity,

Deleted: In order to focus on the modeling and algorithm aspects, we employed two simplified geometries with axis-aligned fibers.

Acknowledgements

The authors gratefully acknowledge financial support by the Theo Rossi di Montelera Foundation, the Metis Foundation Sergio Mantegazza, the Fidinam Foundation, and the Horten Foundation. This work was also supported by the Swiss National Science Foundation, project 205321_149828 "A Flexible High Performance Approach to Cardiac Electromechanics".

References

1. Potse, M., Dubé, B., Richer, J., Vinet, A., & Gulrajani, R. M. A comparison of monodomain and bidomain reaction-diffusion models for action potential propagation in the human heart. *Biomedical Engineering, IEEE Transactions on*, *53*(12), pp. 2425-2435, (2006).

2. Augustin, C.M. and Neic, A. and Liebmann, M, and Prassl, A.J. and Niederer, S.A. and Haase, G. and Plank, G.; ***Anatomically accurate high resolution modeling of human whole heart electromechanics: A strongly scalable algebraic multigrid solver method for nonlinear deformation***; *J. Comp Physics; 305, pp. 622-646, (2016).*

3. Keller, D. U. J. and Jarrousse, O. and Fritz, T. and Ley, S. and Dössel, O. and Seemann, G.; ***Impact of physiological ventricular deformation on the morphology on the t-wave: a hybrid, static-dynamic approach***, *IEEE Trans Biomed Eng., vol 58(7), pp. 2019-2119, (2011).*

Moved (insertion) [2]

Formatted: List Paragraph, Numbered + Level: 1 + Numbering Style: 1, 2, 3, … + Start at: 1 + Alignment: Left + Aligned at: 0 cm + Indent at: 0.4 cm, Don't hyphenate

Deleted: ¶

Formatted: Font: (Default) Vancouver, 14 pt, Font color: Text 1, Subscript

4.

5. Smith, N.P. and Buist, M.L and Pullan, A.J.; ***Altered T wave dynamics in a contracting cardiac model; J. Cardiovasc Electrophysol.*** *14 (Suppl):S203-9, (2003).*

6. Oliveira, B.L. and Rocha, B.M. and Barra, L.P.S. and Toledo, E.M. and Sundnes, J., and Weber dos Santos, R.; ***Effects of deformation on transmural dispersion of repolarization using in silico models of human left ventricle wedge****; Int. J. Numer. Meth. Biomed. Engng. , Published online in Wiley Online Library, DOI: 12.1002/cnm 2570, (2013).*

7. Cluitmans, M.J.M. and Peeters, R.L.M. and Westra. R.L. and P.G.A. Volders; ***Noninvasive reconstruction of cardiac electrical activity: update on current methods, applications and challenges****; Neth Heart j, DOI 10.1007/s12471-015-0690-9, (2015).*

8. Pezzuto, S and Hake J and Sundnes J,; ***Space–discretization error analysis and stabilization schemes for conduction velocity in cardiac electrophysiology;*** *Int. J. Numer. Meth. Biomed. Engng. DOI: 10.1002/cnm.2762, (2016).*

9. Dickopf, T. and Krause R. ***; Evaluating local approximations of the L2-orthogonal projection between non-nested finite element spaces****. Technical Report 2012-01, Institute of Computational Science, University of Lugano, (2012).*

10. Krause, R. and Zulian, P.; ***A Parallel Approach to the Variational Transfer of Discrete Fields between Arbitrarily Distributed Finite Element Meshes****; ICS Preprint, 201502 (2015), in revision at SISC;* http://icsweb.inf.unisi.ch/preprints/preprints/file201502.pdf

11. Colli Franzone, P. and Pavarino, L.F. and Scacchi, S.; ***Parallel multilevel solvers for the cardiac electro-mechanical coupling;*** *Applied Numerical Mathematics, 95, (Nov. 2014).*

12. Grillo, A. and Giverso, C. and Favino, M. and Krause, R. and Lampe, M. and Wittum, G.; ***Mass Transport in Porous Media With Variable Mass;*** *Numerical Analysis of Heat and Mass Transfer in Porous Media, 27-61 (2012).*

13. Colli Franzone, P. and Pavarino, L.F. and Scacchi, S.; ***Bioloelectrical effects of mechanical feedbacks in a strongly coupled cardiac electro-mechanical model****; Mathematical Models and Methods in Applied Sciences, Vol.26, No:1, pp. 27-57 , (2016).*

14. Richardson, G. and Chapman, J.; ***Derivation of the Bidomain equations for a beating heart with a general microstructure****; SIAM J. APPL. MATH.; Vol 71, No 3, pp.657—675 (2011).*

15. Land,S. et al.; ***Verification of Cardiac Mechanics Softwares****; Proceedings Royal Society A. (2015).*

16. Nash, M. P. and Panfilov, A.V.; ***Electromechanical model of excitable tissue to study reentrant cardiac arrhythmias****, Progress in Biophysics and Molecular Biology 85, pp. 501-522, (2004).*

17. Guccione, J. M. and Costa, K.D. and McCulloch, A.D.; ***Finite element stress analysis of left ventricular mechanics in the beating dog heart;*** *J Biomech, 28(10): 1167-77, (Oct. 1995).*

18. Bonet, J. and Wood, R.D.; ***Nonlinear Continuum Mechanics for Finite Elements Analysis****; Cambridge University Press, 1997, (2008 2nd Edition).*

Moved up [2]: Potse, M., Dubé, B., Richer, J., Vinet, A., & Gulrajani, R. M. **A comparison of monodomain and bidomain reaction-diffusion models for action potential propagation in the human heart**. *Biomedical Engineering, IEEE Transactions on, 53*(12), pp. 2425-2435, (2006).¶

Deleted: <#>Augustin, C.M. and Neic, A. and Liebmann, M. and Prassl, A.J. and Niederer, S.A. and Haase, G. and Plank, G.; ***Anatomically accurate high resolution modeling of human whole heart electromechanics: A strongly scalable algebraic multigrid solver method for nonlinear deformation****: J. Comp Physics; 305, pp. 622-646, (2016).*¶

Deleted: and

Formatted: Font: Not Italic

Moved (insertion) [1]

Deleted: ¶

Formatted: Font: Not Italic

Deleted: (vecchio 17)

Formatted: Font: (Default) Vancouver, 14 pt

Formatted: Font: (Default) Vancouver, 14 pt, Italic

Formatted: Font: (Default) Vancouver, 14 pt

Deleted: ¶

¶

Formatted: Font: (Default) Vancouver, 14 pt

Deleted: ¶

Moved up [1]: Colli Franzone, P. and Pavarino, L.F. and Scacchi, S.; ***Bioloelectrical effects of mechanical feedbacks in a strongly coupled cardiac electro-mechanical model****: Mathematical Models and Methods in Applied Sciences, Vol.26, No:1, pp. 27-57 , (2016).*¶

Formatted: Font: (Default) Vancouver, 14 pt

Formatted: Font: (Default) Vancouver, 14 pt, Italic

Formatted: Font: (Default) Vancouver, 14 pt

Formatted: Font: Not Italic

19. Weber Dos Santos, R. and Campos F.O. and Ciuffo, L.N. and Nygren, A. and Giles, W. and Koch, H.; ATX-II ***Effects on the Apparent Location of M Cells in a Computational Model of a Human Left Ventricular Wedge***; *J Cardiovasc. Electroph. , Vol 17, Isuue Supplement s1, pp. s86-s95, (2006).*

20. Plonsey, R.; ***Volume Conductor Fields of Action Currents;*** *Biophys J. 4(4); pp. 317-328, (Jul. 1964).*

21. Niederer, S. A. and Kerfoot, E. and Benson, A. P. and Bernabeu, M. O. and Bernus, O. and Bradley, C. et al.; ***Verification of cardiac tissue electrophysiology simulators using an N-version benchmark;*** ***Philosophical transactions.*** *Series A, Mathematical, physical, and engineering sciences, 2011, 369 (1954), pp. 4331—4351* http://europepmc.org/articles/PMC3263775

22. Bueno Orovio, A. and Cherry E.M. and Fenton, F.H.; **Minimal model of human ventricular action potentials in tissue**; J. Theor. Biol., 253(3). (Aug. 2008).

23. Augustin, C.M. and Crozier, A. Karabelas, E. and Neic, A. and Prassl, A.J. and Plank, G.; ***Simulating patient-specific whole heart electromechanics with efficient algebraic multigrid preconditioners;*** *International Symposium and Winter-School of Modeling, Adaptive Dicretizations and Solvers for Fluid-Structure Interaction; (Jan. 11-15, 2016).*

24. Gaston, D. R. and Permann, C. J. and Peterson, J. W. and Slaughter, E. and Andrs, D. and Wang, Y. et al; **Physics-based multiscale coupling for full core nuclear reactor simulation;** Annals of Nuclear Energy, Special Issue on Multi-Physics Modelling of LWR Static and Transient Behaviour, vol. 84, pp. 45-54 (Oct. 2015).

25. Leenders, G. E. and Lumens, J. and Cramer, M. J. and De Boeck, B. W. and Doevendans, P.A. and Delhaas, T. et al. **Septal deformation patterns delineate mechanical dyssynchrony and regional differences in contractility analysis of patient data using a computer model;** Circulation: Heart Failure, 5, pp. 87—96 (2012)

26. Whiteley, J. P., Bishop, M. J., & Gavaghan, D. J. **Soft tissue modelling of cardiac fibres for use in coupled mechano-electric simulations;** *Bulletin of mathematical biology, 69*(7), 2199-2225, (2007).

27. Ambrosi, D., & Pezzuto, S. **Active stress vs. active strain in mechanobiology: constitutive issues;** *Journal of Elasticity, 107*(2), 199-212, (2012).

28. Villongco, C. T., Krummen, D. E., Stark, P., Omens, J. H., & McCulloch, A. D. **Patient-specific modeling of ventricular activation pattern using surface ECG-derived vectorcardiogram in bundle branch block;** *Progress in biophysics and molecular biology, 115*(2), pp. 305-313, (2014).

29. Trayanova, N. A., Constantino, J., & Gurev, V. **Electromechanical models of the ventricles**: *American Journal of Physiology-Heart and Circulatory Physiology, 301*(2), H279-H286, (2011).

Formatted: Widow/Orphan control

Deleted: ¶

Formatted: Font: (Default) Vancouver, 14 pt

Deleted: <#>Richardson, G. and Chapman, J.; ***Derivation of the Bidomain equations for a beating heart with a general microstructure***; *SIAM J. APPL. MATH.; Vol 71, No 3, pp.657—675 (2011).*¶

Formatted: Font: Bold

Formatted: Font: Not Bold

Deleted: <#>Weber Dos Santos, R. and Campos F.O. and Ciuffo, L.N. and Nygren, A. and Giles, W. and Koch, H.; ATX-II ***Effects on the Apparent Location of M Cells in a Computational Model of a Human Left Ventricular Wedge***; *J Cardiovasc. Electroph. , Vol 17, Isuue Supplement s1, pp. s86-s95, (2006).*¶

Plonsey, R.; ***Volume Conductor Fields of Action Currents;*** *Biophys J. 4(4); pp. 317-328, (Jul. 1964).*¶

Villongco, C. T., Krummen, D. E., Stark, P., Omens, J. H., & McCulloch, A. D. **Patient-specific modeling of ventricular activation pattern using surface ECG-derived vectorcardiogram in bundle branch block;** *Progress in biophysics and molecular biology, 115*(2), 305-313, (2014).¶

Trayanova, N. A., Constantino, J., & Gurev, V. **Electromechanical models of the ventricles**: *American Journal of Physiology-Heart and Circulatory Physiology, 301*(2), H279-H286, (2011).¶

Formatted: Indent: Left: 0.4 cm, No bullets or numbering

Figures

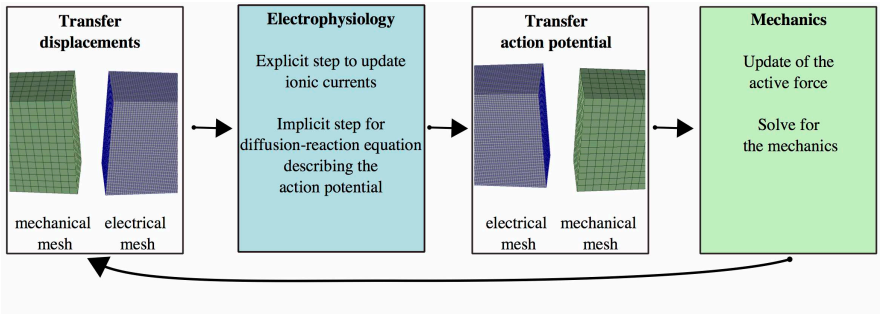

Figure 1. Representation of the staggered solution algorithm for the electro-mechanical coupled problem. At each iteration, first displacements are transferred to the electrophysiology solver. Here the potential at the new time step is computed on a finer mesh. Then the updated potential is transferred to the mechanical solver in order to compute the active force and the resulting new configuration.

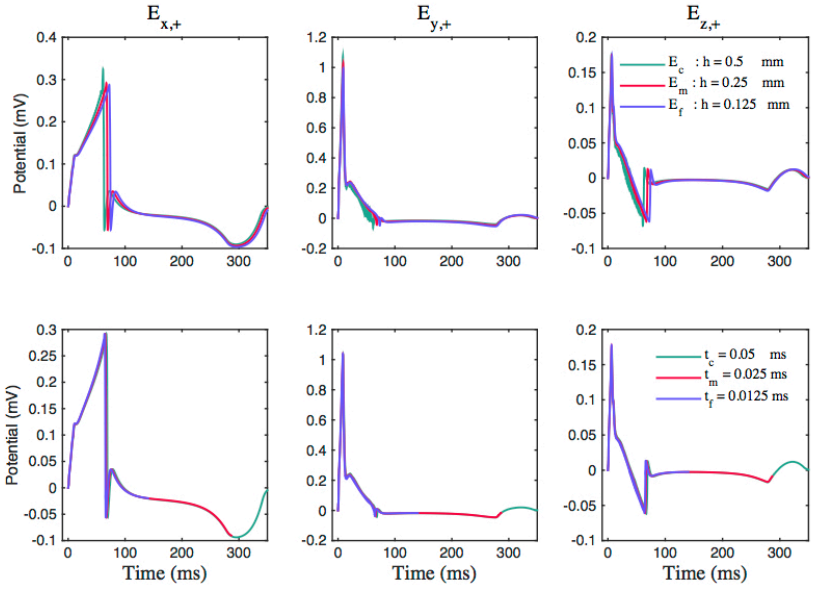

Figure 2 Top row: convergence of the unipolar pseudo-ECGs under spatial mesh refinement, employing a temporal step-size t_f. Bottom row: convergence of the unipolar pseudo-ECGs under temporal step-size refinement, employing the mesh E_f.

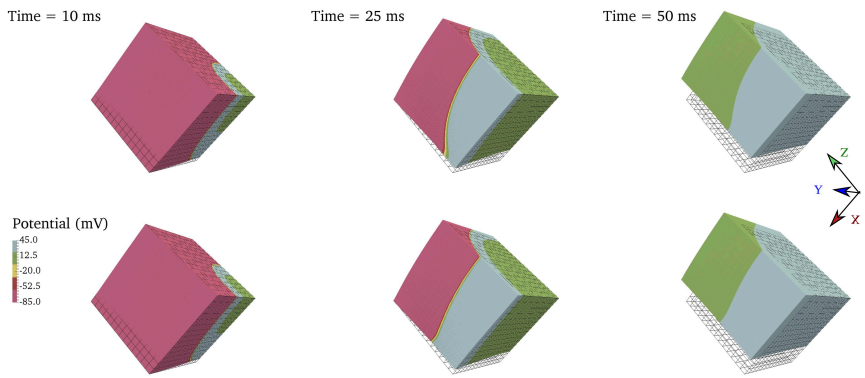

Figure 3. Test case A: electromechanical activation of a cube with fibers aligned along the x-axis using the mono-directional (static-dynamic) coupling (top row) and using a fully-coupled approach (bottom row). The reference mechanical mesh is reported.

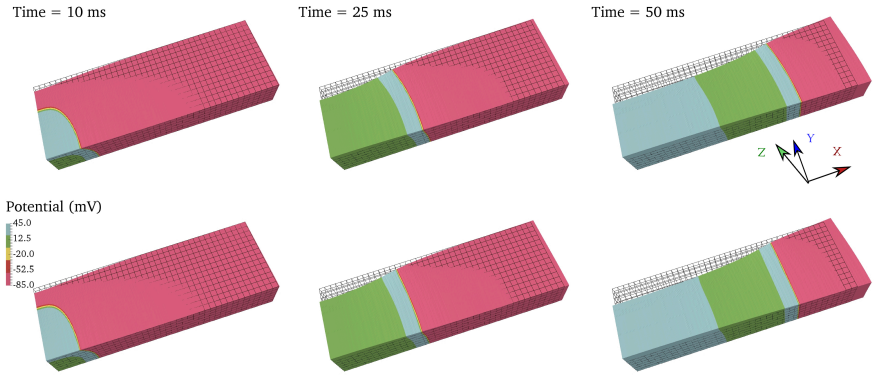

Figure 4. Test case C: electromechanical activation of a tissue slab with fibers aligned along the y-axis using the mono-directional (static-dynamic) coupling (top row) and using a fully-coupled approach (bottom row). The reference mechanical mesh is reported.

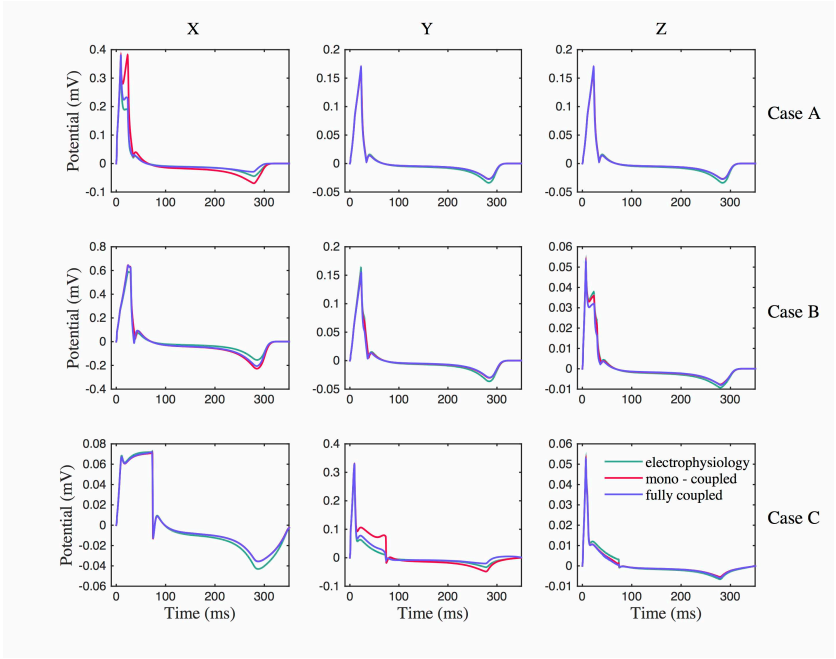

Figure 5. Simulated pseudo-ECGs for the different test cases (by row). Bipolar signals are computed between the far electrodes along the three coordinate axes (by column).

Tables

		X_{p1} = 0.2 mm	X_{p2} = 0.3 mm	X_{p3} = 0.5 mm	X_{p4} = 0.7 mm
CASE A	Electrophysiology Mono - coupled	6.5 ms	12.5 ms	24.0 ms	32.0 ms
	Fully -coupled	6.5 ms	13.0 ms	24.5 ms	33.5 ms

		X_{p1} = 0.5 mm	X_{p2} = 1.0 mm	X_{p3} = 1.5 mm	X_{p4} = 2.0 mm
CASE B	Electrophysiology Mono - coupled	8.0 ms	18.5 ms	29.5 ms	39.0 ms
	Fully -coupled	8.0 ms	18.5 ms	28.5 ms	37.0 ms
CASE C	Electrophysiology Mono - coupled	16.0 ms	36.0 ms	56.0 ms	74. 5 ms
	Fully -coupled	16.0 ms	36.0 ms	55.5 ms	72.5 ms

Table 1. Comparison of the activation times for the different test cases and for the different approaches. Pure electrophysiology and mono-directional coupling are characterized by the same activation times because of their mathematical model. In column we report the x-coordinate of the chosen point on the selected diagonal.